Electronic Supplementary Material (ESI) for Polymer Chemistry

Calix[4]pyrogallolarenes as novel high temperature inhibitors of oxidative degradation of polymers

Przemysław Ziaja,[a] Katarzyna Jodko-Piórecka,[a] Rafał Kuźmicz,[b] Grzegorz Litwinienko[a*]

[a] University of Warsaw, Faculty of Chemistry, Pasteura 1, 02-093 Warsaw, Poland
[b] Faculty of Pharmacy, Medical University of Warsaw, Banacha 1, 02-097 Warsaw, Poland

ELECTRONIC SUPPLEMENTARY INFORMATION

TABLE OF CONTENTS

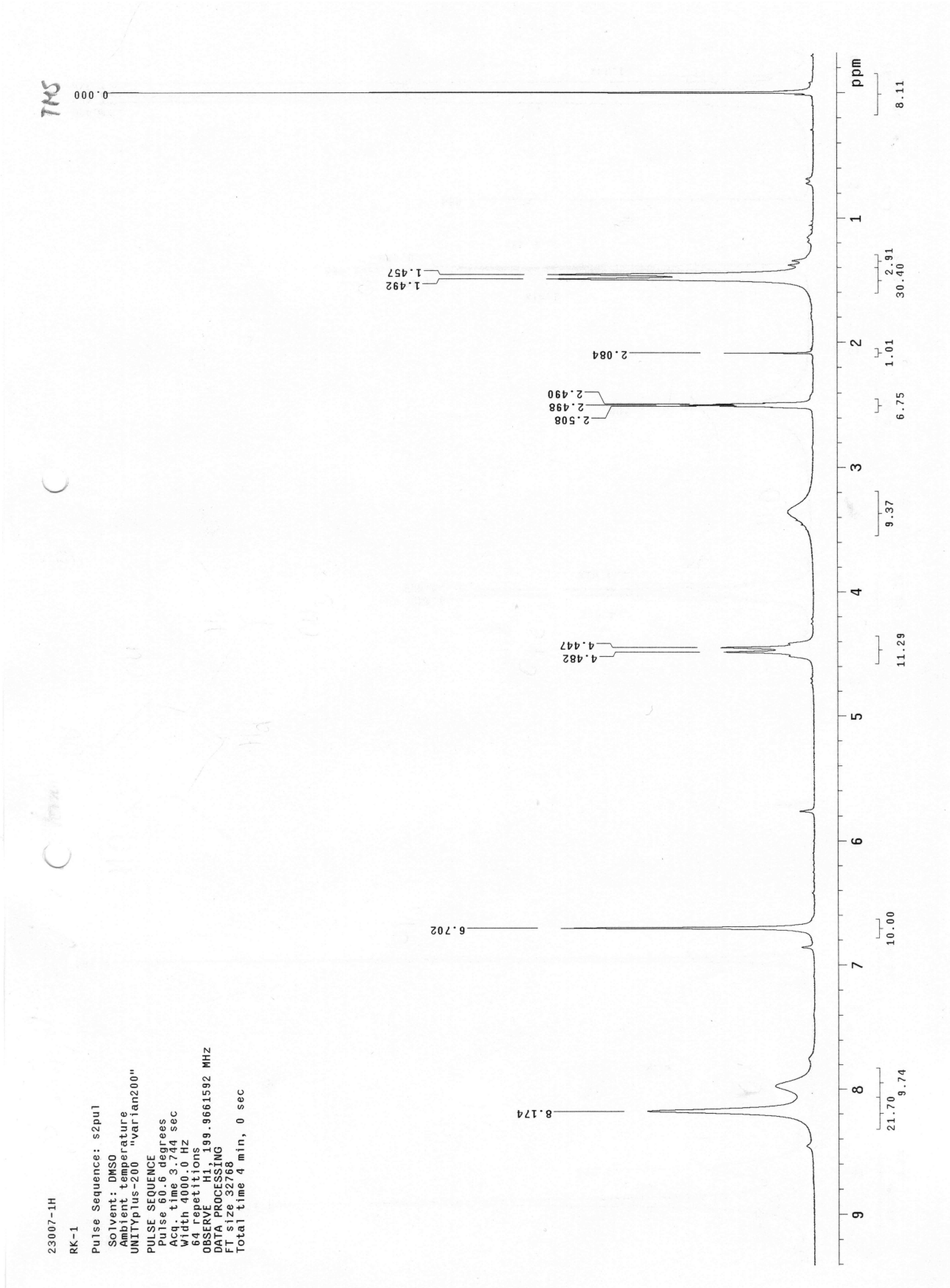

Figure S1. ^{1}H-NMR spectrum of C-methylcalix[4]pyrogallolarene recrystallized from acetone (200 MHz, DMSO-d_6)

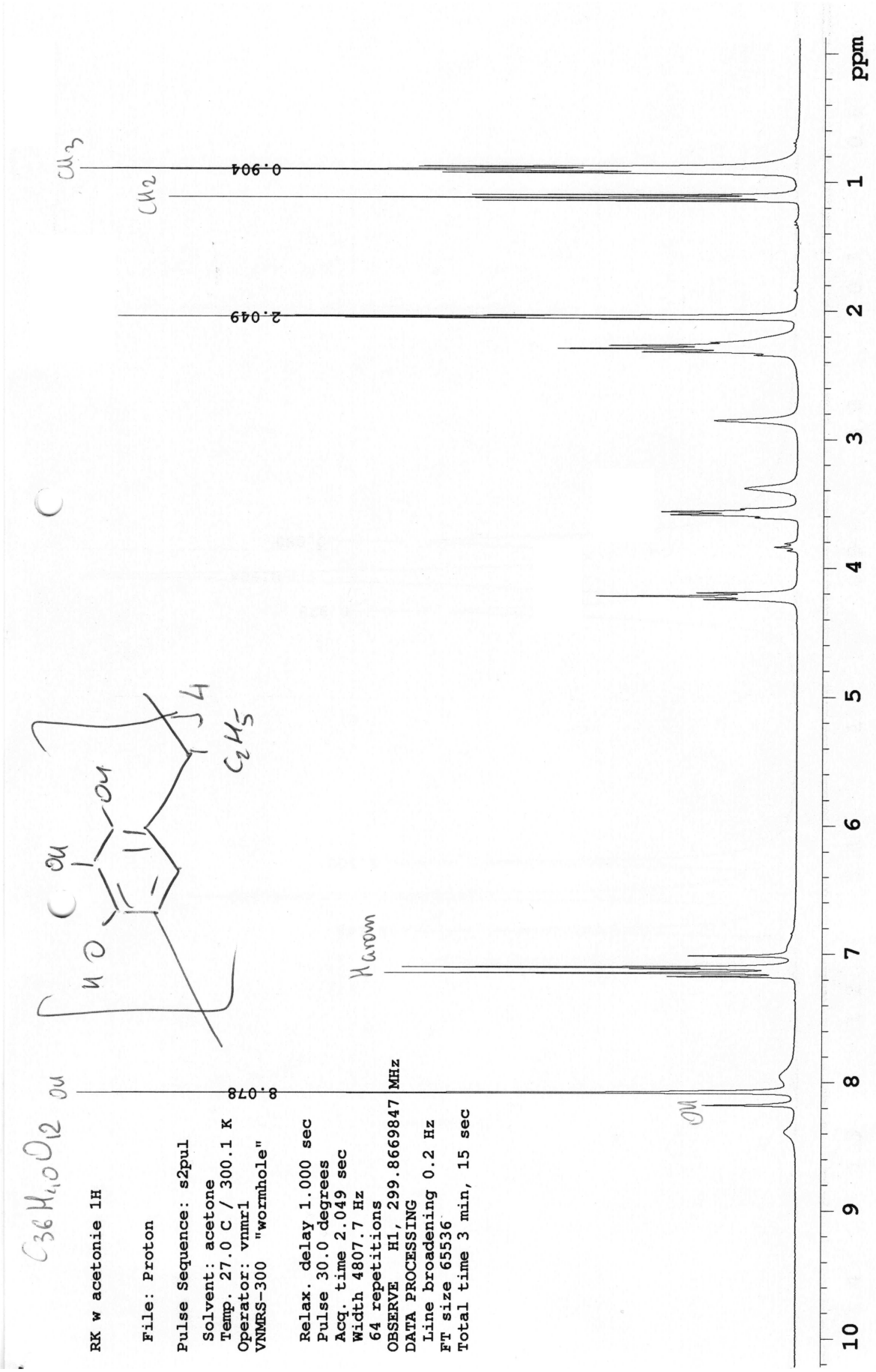

Figure S2. ^{1}H-NMR spectrum of C-ethylcalix[4]pyrogallolarene (200 MHz, acetone-d_6)

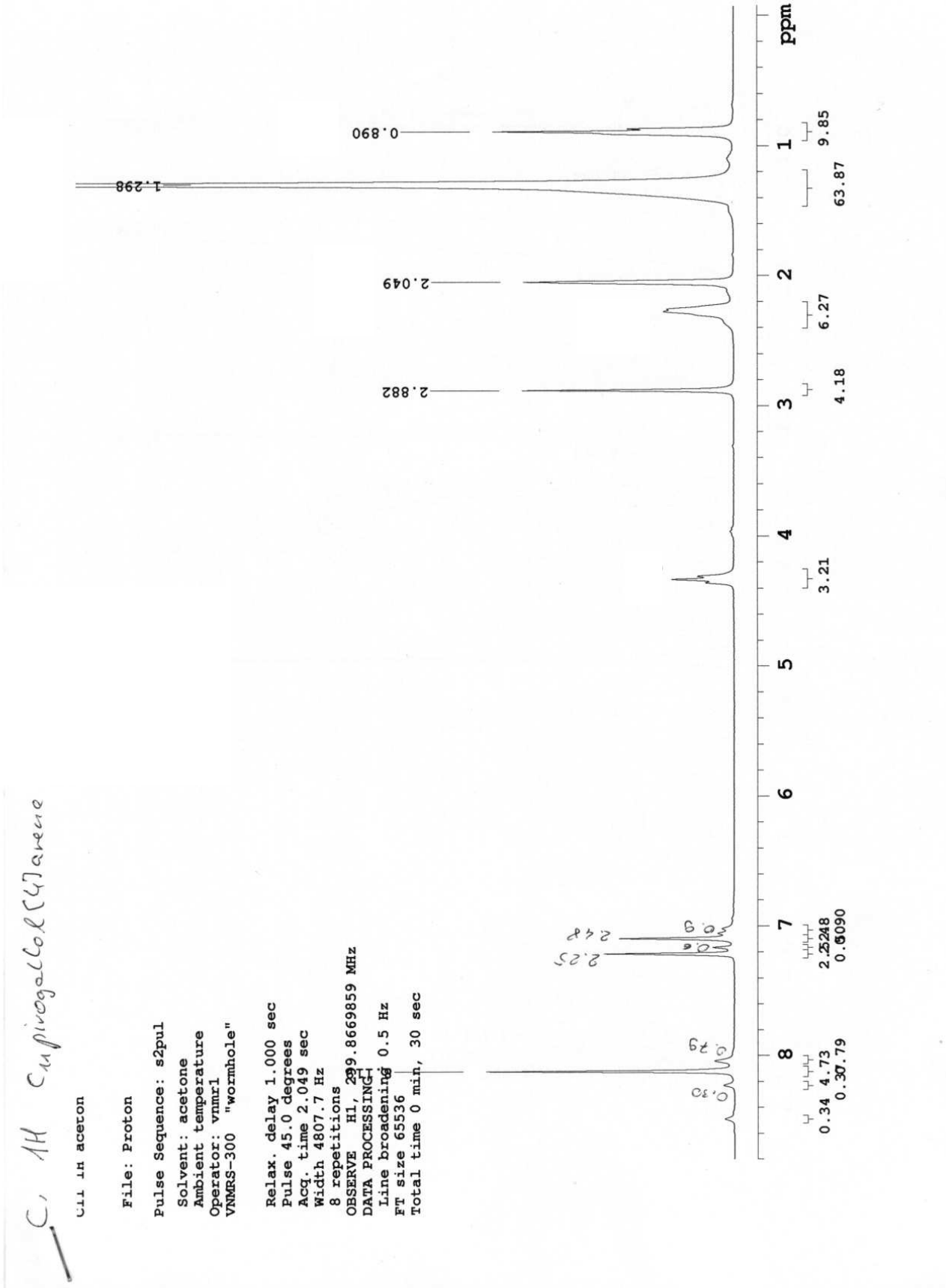

Figure S3. ^{1}H-NMR spectrum of C-undecylcalix[4]pyrogallolarene (200 MHz, acetone-d_6)

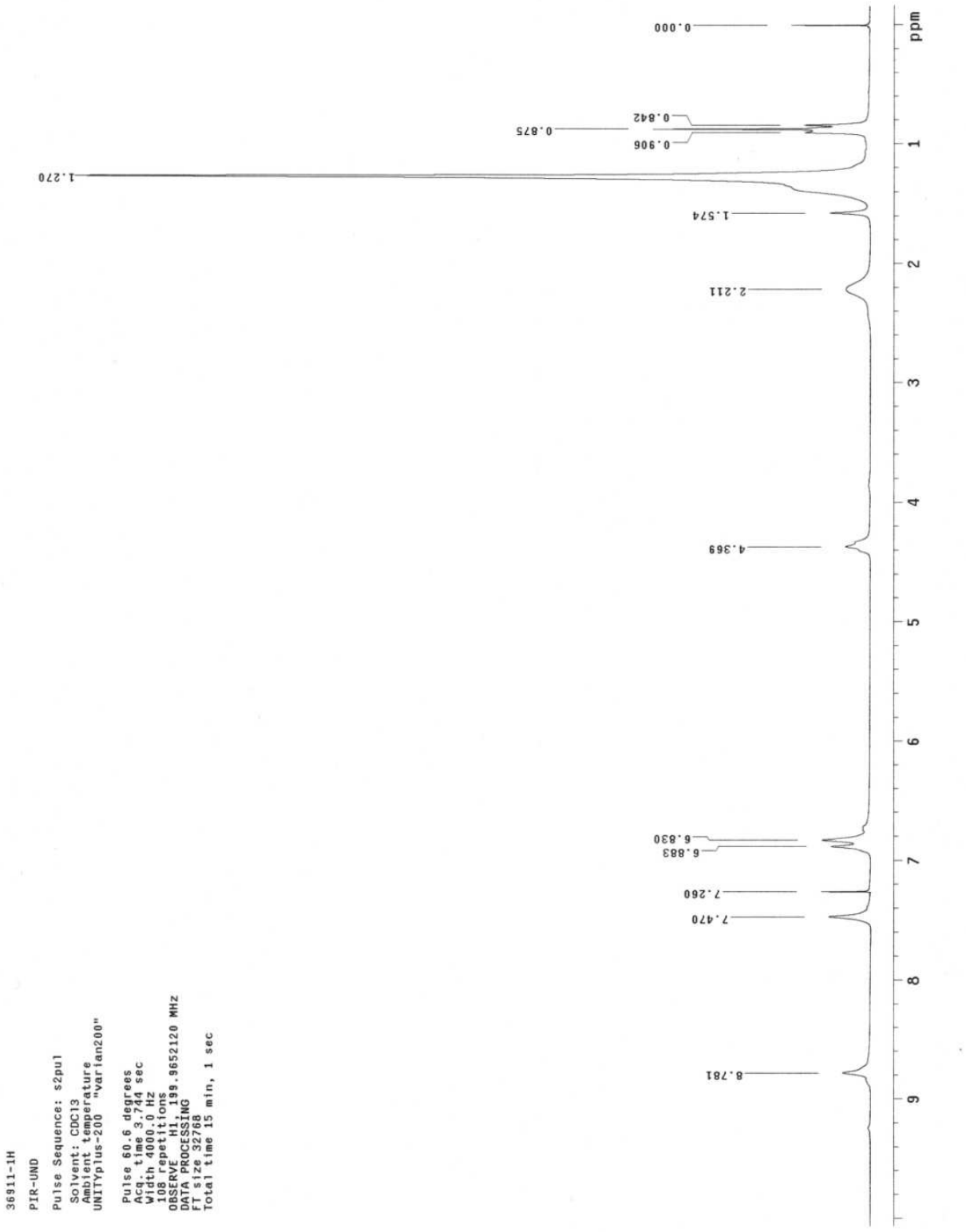

Figure S4. ^{1}H NMR spectrum of C-undecylcalix[4]pyrogallolarene heated isothermally over 3 hours at 220°C under vacuum ($CDCl_3$). The spectrum was recorded immediately after isothermal heating.

Experimental procedures and the determination of kinetic parameters of thermo-oxidative decomposition of HDPE as well as polymeric composites.

Materials.

High density polyethylene (HDPE for the use in spectroscopy, density 0.96 g/cm^{-3}, melting point 132-134ºC, powder) was obtained from Merck and used as received.
C- methylcalix[4]pyrogallolarene, C-ethylcalix[4]pyrogallolarene, C-undecylcalix[4]pyrogallolarene were synthesized according to the modified procedure described by Aoyama et al. (Aoyama, Y.; Tanaka, Y.; Sugahara, S. *J. Am. Chem. Soc.* **1989**, *111*, 5397-5404) and by Gerkensmeier et al. (Gerkensmeier, T.; Agena, C.; Iwanek, W.; Fröhlich, R.; Kotila, S.; Näther, C.; Mattay, J.; *Z. Naturforsch., B: Chem. Sci.* **2001**, *56*, 1063-1073). Pyrogallol (1,2,3-trihydroxybenzene) was purchased from Sigma-Aldrich (99% of purity). All aliphatic aldehydes: ethanal, propanal, dodecanal (98% of purity) and solvents: ethanol, acetone (99+%) were used without further purification.

Each of the macrocyclic tetramers was obtained in an acid catalyzed condensation reaction between pyrogallol (1,2,3-trihydroxybenzene) and an aliphatic aldehyde. Firstly, 40 mmol of pyrogallol was dissolved in 25 cm^3 of ethanol in round-bottom flask immersed in an ice bath, then 6.0 cm^3 of concentrated hydrochloric acid was added. After that the solution of aliphatic aldehyde containing 40 mmol of aldehyde dissolved in 15 cm^3 of cold ethanol was added dropwise to the mixture in the flask. When the solution of aldehyde was added completely, the temperature was allowed to rise until 40°C. The reaction was carried out at 40°C during 24 hours under reflux, continuous stirring and the flow of helium. When the formation of a precipitate was not observed, the mixture was cooled and concentrated under reduced pressure on a vacuum evaporator. The obtained precipitate was washed several times with ethanol, crystallized and dried. The typical yield of the synthesis of pyrogallolarenes was 70-90%.

Proton NMR spectra of C-R-alkylcalix[4]pyrogallolarenes were recorded on a Varian UnityPlus spectrometer at 199,96 MHz and 298K. The spectra were done in DMSO-d_6, acetone-d_6 or in $CDCl_3$ and are listed as δ values in ppm (versus TMS).

Proton NMR spectrum of C-methylcalix[4]pyrogallolarene recrystallized from acetone (200 MHz, DMSO-d_6, Figure S1) : 1.47 (d, 12 H, C*H*$_3$, J = 7.0 Hz), 4.46 (q, 4H, methine C*H*, 7.0 Hz), 6.70 (s, 4H, aromatic C*H*), 7.97 (bs, 4H, O*H*), 8.17 (bs, 8H, O*H*), 2.08 (s, acetone C*H*$_3$), 2.50 – solvent residual peak, 3.35 (s, 4H, water).

Proton NMR spectrum of C-ethylcalix[4]pyrogallolarene (200 MHz, acetone-d_6, Figure S2): 0.90 (t, 12 H, C*H*$_3$, J = 4.8 Hz), 2.30 (m, 8 H, C*H*$_2$), 4.22 (t, 4H, methine C*H*, J = 5.3 Hz), 7.01-7.17 the overlapping of the signals (s, 4H, aromatic C*H* overlaps with the signal of 4H, O*H*), 7.95, 8.08, 8.16 and 8.36 (s, 8H, O*H*), 1.12 (t, 6H, C*H*$_3$ from ethanol), 2.05 – solvent residual peak, 3.38 (s, 2H, O*H* from ethanol), 3.57 (q, 4H, C*H*$_2$ from ethanol), 2.85 (s, 2H, water).

Proton NMR spectrum of C-undecylcalix[4]pyrogallolarene (200 MHz, acetone-d_6, Figure S3): 0.89 (t, 12H, C*H*$_3$), 1.30 (m, 72H, CH_2(C*H*$_2$)$_9$$CH_3$), 2.28 (m, 8H, C*H*$_2$($CH_2$)$_9$), 4.33 (t, 4H, methine C*H*, J = 5.0 Hz), 7.10 (s, 4H, aromatic C*H*), 7.21 (s, 4H, O*H*), 8.04, 8.12, 8.23 and 8.49 (s, 8H, OH), 2.05 – solvent residual peak, 2.88 (s, 4H, water).

Proton NMR spectrum of C-undecylcalix[4]pyrogallolarene heated isothermally over 3 hours at 220°C (200 MHz, $CDCl_3$, Figure S4): 0.87 (t, 12H, C*H*$_3$, J = 6.4 Hz), 1.27 (m, 72H, CH_2(C*H*$_2$)$_9$$CH_3$), 2.21 (m, 8H, C*H*$_2$($CH_2$)$_9$), 4.37 (t, 4H, methine C*H*), 6.83 (s, 4H, aromatic C*H*), 6.88 (s, 4H, O*H*), 7.47 (s, 4H, OH), 8.78 (s, 4H, OH), 7.26 – solvent residual peak, 1.57 (s, 6H, water).

Before pyrogallolarenes were further applied in the preparation of the polymeric composites, all pyrogallolarenes were heated isothermally at 220°C over 3 hours under vacuum in order to obtain desolvated samples. Additional TG measurements revealed (see Figure S6), that all C-R-calix[4]resorcinarenes did not contain solvents.

C-R-alkylcalix[4]pyrogallolarenes were identified by means of ^{1}H-NMR analysis and the signals on the NMR spectra are in agreement with literature data for C-R-calix[4]pyrogallolarenes (in hexameric assemblies) reported by: Kulikov, O. V.; Rath, N. P.; Zhou, D.; Carasel, I. A.; Gokel, G. W. *New. J. Chem.* **2009**, 33, 1563-1569 and Avram, L.; Cohen, Y. *J. Am. Chem. Soc.* **2004**, 126, 11556-11563 and

Gerkensmeier, T.; Agena, C.; Iwanek, W.; Fröhlich, R.; Kotila, S.; Näther, C.; Mattay, J.; *Z. Naturforsch., B: Chem. Sci.* **2001**, *56*, 1063-1073.

Preparation of the polyethylene composites.

HDPE (0.50 ± 0.01 g) was precisely ground in a mortar and calculated volume of acetone solution of a phenol derivative was subsequently added with continuous grinding of the mixture until the homogeneous powder was obtained. The composite was moved into Petri dish and left for one hour to evaporate acetone. After that time the weight of sample was stable. TG measurements indicated that removal of acetone was complete.

Apparatus and methods.

Thermogravimetric measurements in non-isothermal mode were carried out with a DuPont 951 termobalance (precision, ±0.4%; minimal mass, 0.02 mg) under nitrogen flow 6 dm^3/h and in a platinum vessel. In a typical TG measurement a sample (~5 mg) was heated at 5 K/min from 50 to 600°C. The decomposition of a model compound – calcium oxalate monohydrate was carried out before typical TGA measurements.

The series of DSC measurements in non-isothermal mode were carried out by means of DSC apparatus DuPont 910 differential scanning calorimeter equipped with normal pressure cell (oxygen atmosphere with oxygen flow 6 dm^3/h) and DuPont 9900 thermal analyzer. The DSC apparatus was calibrated with high-purity indium standard and an empty aluminum pan was used as a reference. TA Instruments Software (General V4.01) was used for data collection and for the determination of the temperatures of the extrapolated start of oxidation (T_e). In a typical DSC measurement a sample of composite (3-3.5 mg ± 0.1 mg) was heated from 70 to 300°C in an open aluminum pan at a linear heating rate β and T_e was determined. For the same β the experiment was repeated three times with a new sample to have a mean value of T_e. Then all procedure of DSC measurement was repeated to obtain T_e determined for at least 5-8 different values of β (ranging from 2 to 20 K/min). Thus, a series of T_e's was obtained with each T_e as a mean of three repetitions.

Overall kinetic parameters (E_a –activation energy, Z – pre-exponential factor, k – rate constant at a chosen temperature) of thermo-oxidative degradation of polyethylene's composites were calculated on the basis of the Ozawa-Flynn-Wall method (**derivation of the method is described in Appendix**). For a series of T_e a straight line dependence: $\log\beta = aT_e^{-1} + b$ with the slope $a = -0.4567E_a/R$ and reciprocal $b = -2.315 + \log(ZE_a/R)$ is obtained, thus:

$$E_a = -2.19\ R\ d\log\beta/d(T^{-1})$$

$$\log Z = (b+2.315) - \log(E_a/R)$$

The errors of activation energy (denoted as ± E_a) were estimated on the basis of the standard deviations of the slopes calculated for confidence level 90%.

If Z and E_a are known, the rate constant, $k(T)$, can be calculated from the classical Arrhenius equation:

$$k(T)=Z\exp(-E_a/RT)$$

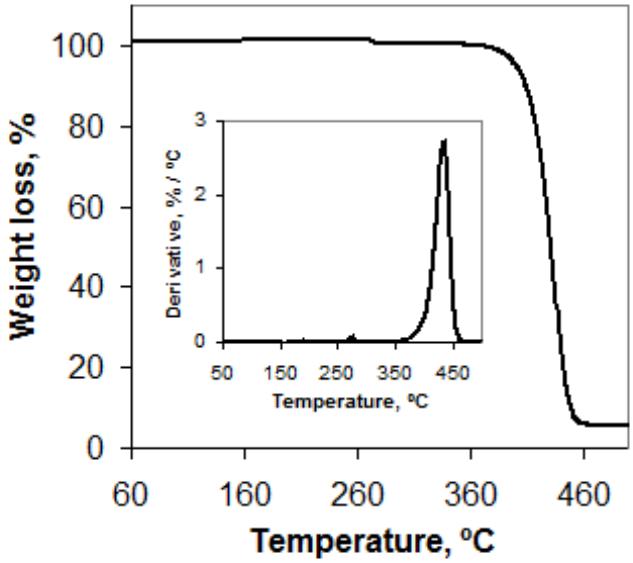

Figure S5. Thermogravimetric measurement of thermal decomposition of neat HDPE (monitored at 5 K/min under nitrogen flow), inset presents a TG derivative with respect to temperature.

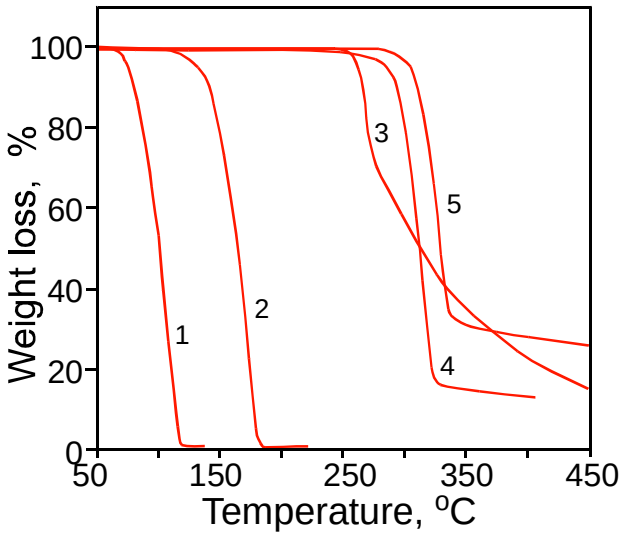

Figure S6. Thermogravimetric curves of thermal decomposition of 2,6-di-tert-butyl-4-methylphenol (1), 1,2,3-trihydroksybenzene (2), C-undecylcalix[4]pyrogallolarene (3) C-ethylcalix[4]pyrogallolarene (4), C-methylcalix[4]pyrogallolarene (5), monitored at 5 K/min under nitrogen.

Table S1. Temperatures of extrapolated start of oxidation (T_e) determined for various heating rates β for oxidation of pure HDPE. Parameters of equation 3 were calculated by OFW method: overall activation energy (E_a) and pre-exponential factor (Z), logarithms of overall rate constants (k, at 150, 200, 250°C) and standard error σ and error for confidence level 90% ($\sigma_{90\%}$).

β / K·min^{-1}	T_e / K	Statistical and kinetic parameters
2.0	452.1	a = -6.98
5.0	465.2	b = 15.72
7.5	470.3	R^2 = 0.9960
10	475.0	σ = 0.18
12.5	478.1	$\sigma_{90\%}$ = 0.33
15	479.8	E_a = 127±6 kJ/mol
17.5	481.6	Z = 7.15·10^{13} s^{-1}
20	483.1	log($k_{150°C}$ /s^{-1}) = -3.61
		log($k_{200°C}$ /s^{-1}) = -1.96
		log($k_{250°C}$ /s^{-1}) = -0.62

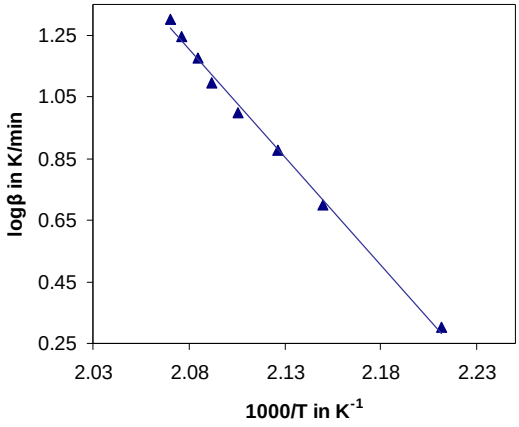

Figure S7. Plot of equation 3 for pure HDPE.

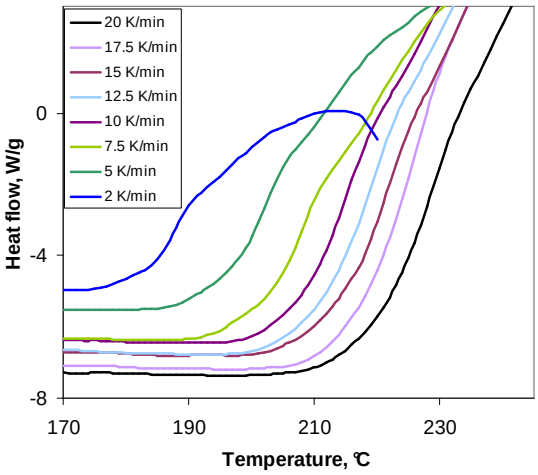

Figure S8. DSC curves of oxidative decomposition of HDPE containing BHT at 0.5% (w/w). All measurements were carried out by DSC in non-isothermal mode at different linear heating rates (β, in $K \cdot min^{-1}$).

Table S2. Temperatures of extrapolated start of oxidation (T_e) determined for various heating rates β for oxidation of HDPE containing 0.5% (w/w) BHT. Parameters of equation 3 were calculated by OFW method: overall activation energy (E_a) and pre-exponential factor (Z), logarithms of overall rate constants (k, at 150, 200, 250°C) and standard error σ and error for confidence level 90% ($\sigma_{90\%}$).

β / $K \cdot min^{-1}$	T_e / K	Statistical and kinetic parameters
2.0	456.05	a = -6.31
5.0	468.15	b = 14.17
7.5	473.74	R^2 = 0.9969
10	479.87	σ = 0.14
12.5	482.9	$\sigma_{90\%}$ = 0.27
15	485.68	E_a = 115±5 kJ/mol
17.5	488.87	$Z = 2.19 \cdot 10^{12}$ s^{-1}
20	491.14	$\log(k_{150°C}/s^{-1}) = -3.62$
		$\log(k_{200°C}/s^{-1}) = -2.12$
		$\log(k_{250°C}/s^{-1}) = -0.91$

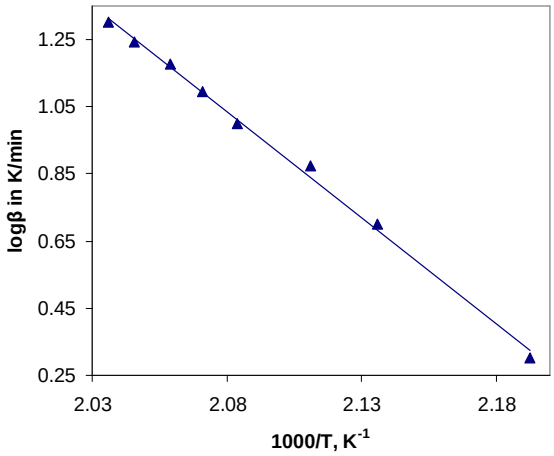

Figure S9. Plot of equation 3 for HDPE containing 0.5% (w/w) of BHT.

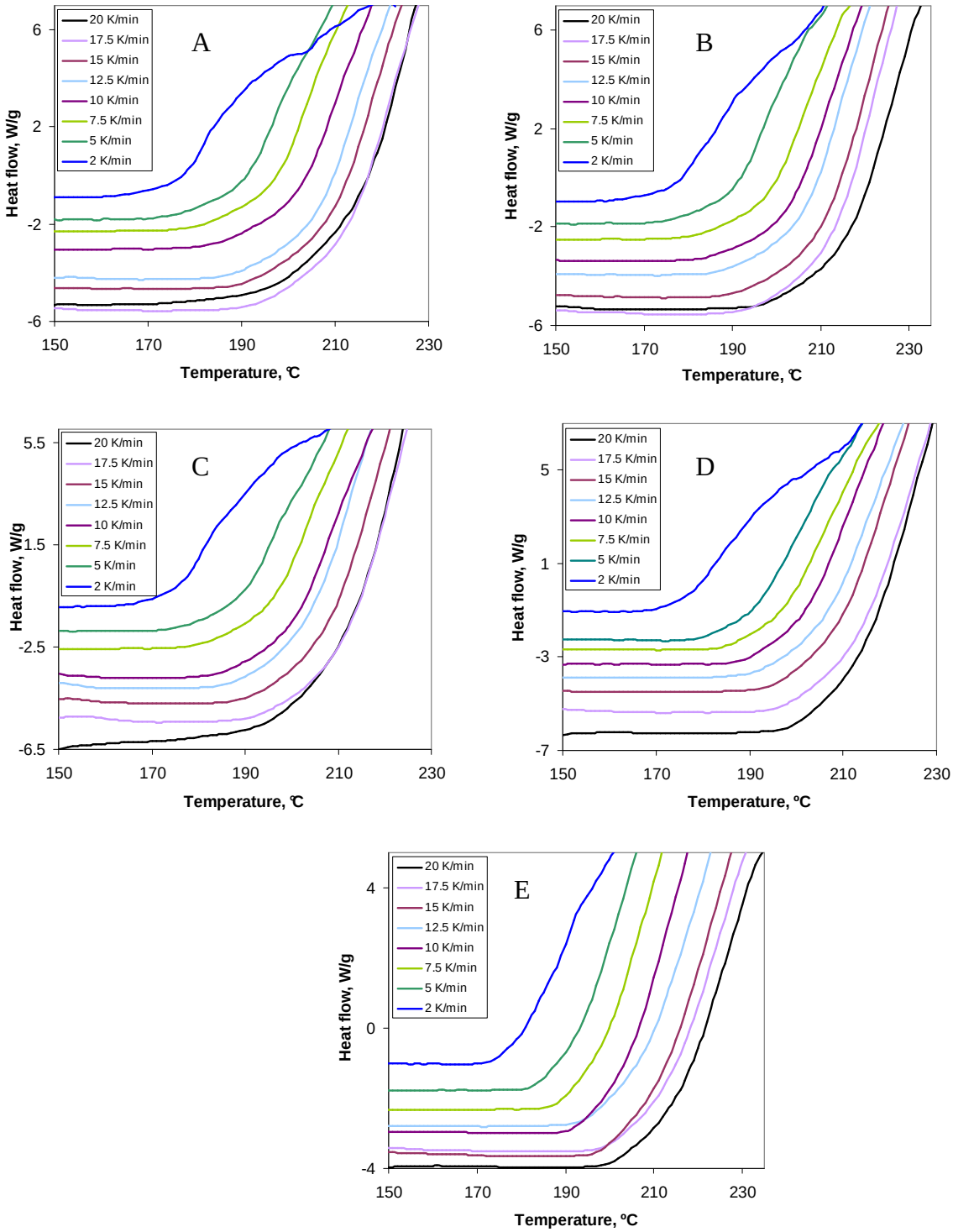

Figure S10. DSC curves of oxidative decomposition of HDPE containing pyrogallol at concentrations (w/w): A) 0.013%, B) 0.026%, C) 0.052%, D) 0.104% E) 0.208%. All measurements were carried out by DSC in non-isothermal mode at different linear heating rates (β, in $K \cdot min^{-1}$).

Table S3. Temperatures of the extrapolated start (T_e, in K) of oxidation of HDPE composites containing pyrogallol. The decomposition was monitored at different linear heating rates (β, in K·min^{-1}).

β / K·min^{-1}	pyrogallol concentration [a]				
	0.013%	0.026%	0.052%	0.104%	0.208%
2	448.4	448.0	446.6	448.7	451.2
5	461.2	461.7	459.6	461.9	463.3
7.5	468.1	468.3	466.2	467.2	468.4
10	472.9	474.0	470.9	472.4	473.8
12.5	476.7	477.1	474.2	475.8	477.0
15	479.5	480.3	477.8	478.7	480.3
17.5	481.7	482.5	480.5	481.8	482.5
20	484.4	485.0	482.4	483.3	484.9

[a] In % (w/w).

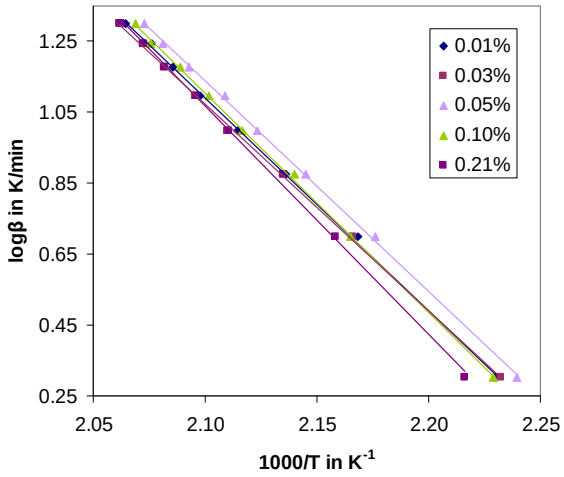

Figure S11. Plots of equation 3 for thermo-oxidation of HDPE composite containing pyrogallol.

Table S4. Parameters of equation 3, overall activation energies (E_a / kJ·mol^{-1}) and logarithms of pre-exponential factors (Z / s^{-1}) and logarithms of the overall rate constants for oxidation at 150°C, 200°C, 250°C (k / s^{-1}) calculated for HDPE / pyrogallol composites. Concentrations of inhibitor in % (w/w).

Concentration of inhibitor	a	b	R^2	E_a [a]	log$Z$	log$k_{(150°C)}$	log$k_{(200°C)}$	log$k_{(250°C)}$
pyrogallol								
0.013	-6.02	13.73	0.9993	110±3	11.92	-3.38	-1.95	-0.79
0.026	-5.83	13.31	0.9993	106±2	11.52	-3.35	-1.97	-0.85
0.052	-5.96	13.65	0.9995	109±2	11.85	-3.32	-1.90	-0.76
0.104	-6.21	14.15	0.9992	113±3	12.33	-3.41	-1.93	-0.74
0.208	-6.45	14.61	0.9979	117±4	12.77	-3.50	-1.96	-0.73

[a] The errors of the activation energy E_a estimated on the basis of the standard deviations of the slopes (listed in column 2) calculated for confidence level 90%.

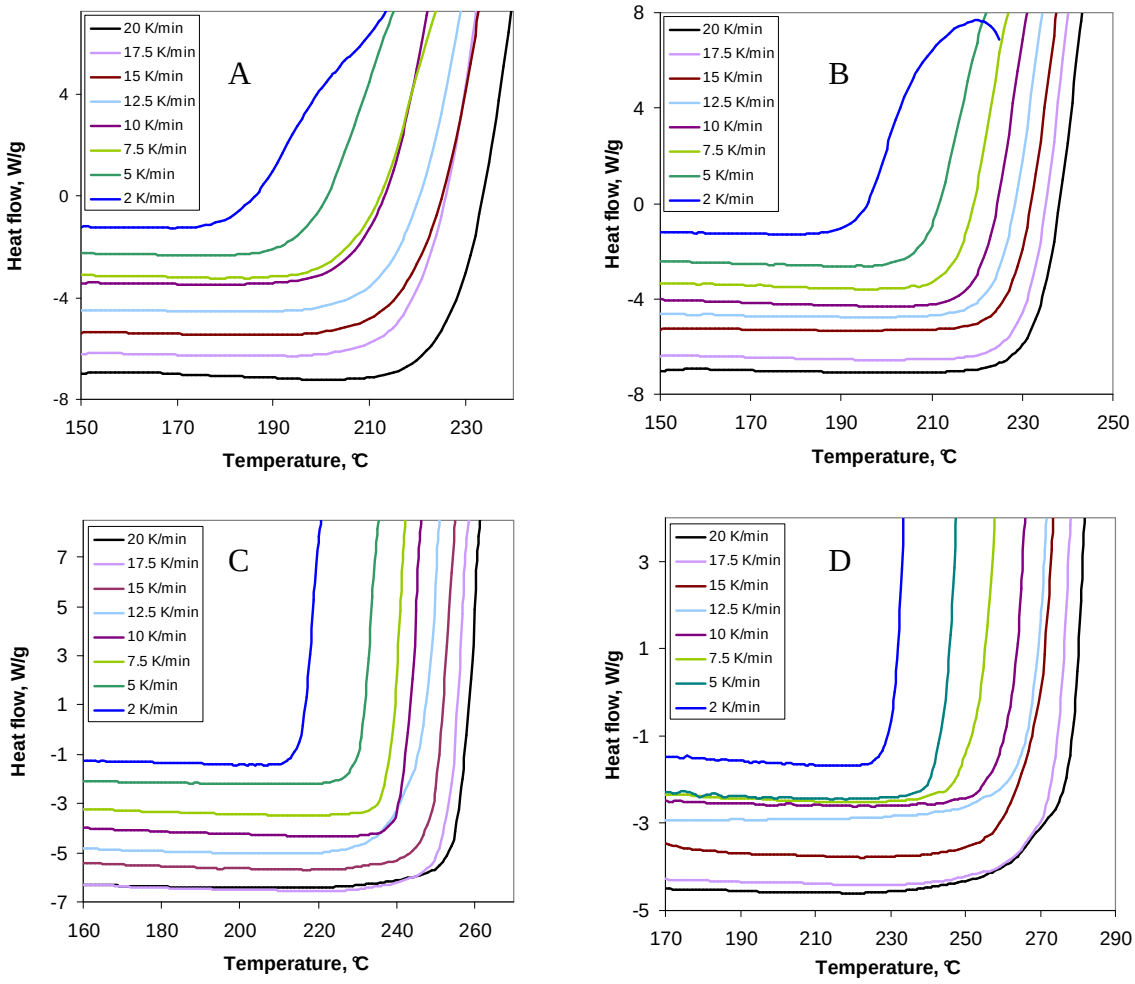

Figure S12. DSC curves of oxidative decomposition of HDPE containing C-methylcalix[4]pyrogallolarene at concentrations (w/w): A) 0.063%, B) 0.127%, C) 0.254%, D) 1.02%. All measurements were carried out by DSC in non-isothermal mode at different linear heating rates (β, in $K \cdot min^{-1}$).

Table S5. Temperatures of the extrapolated start (T_e, in K) of oxidation of HDPE composites containing C-methylcalix[4]pyrogallolarene. The decomposition was monitored at different linear heating rates (β).

β / $K \cdot min^{-1}$	C-methylcalix[4]pyrogallolarene concentration [a]				
	0.063% [a]	0.127%	0.254%	0.508%	1.016%
2	456.0	467.7	489.2	498.0	504.1
5	471.1	482.5	503.8	512.3	516.8
7.5	479.2	489.9	510.9	517.7	526.2
10	482.6	494.4	514.4	522.3	531.8
12.5	487.8	497.5	517.3	525.4	536.7
15	491.1	500.9	521.5	528.7	540.1
17.5	492.5	503.7	525.0	532.2	544.9
20	498.3	506.5	527.3	534.4	548.8

[a] In % (w/w).

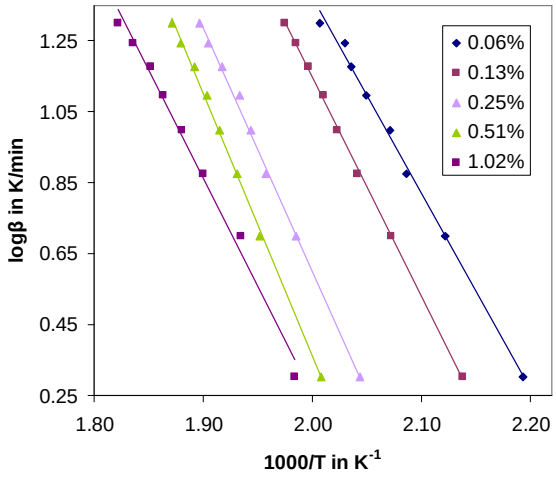

Figure S13. Plots of equation 3 for HDPE composite containing C-methylcalix[4]pyrogallolarene.

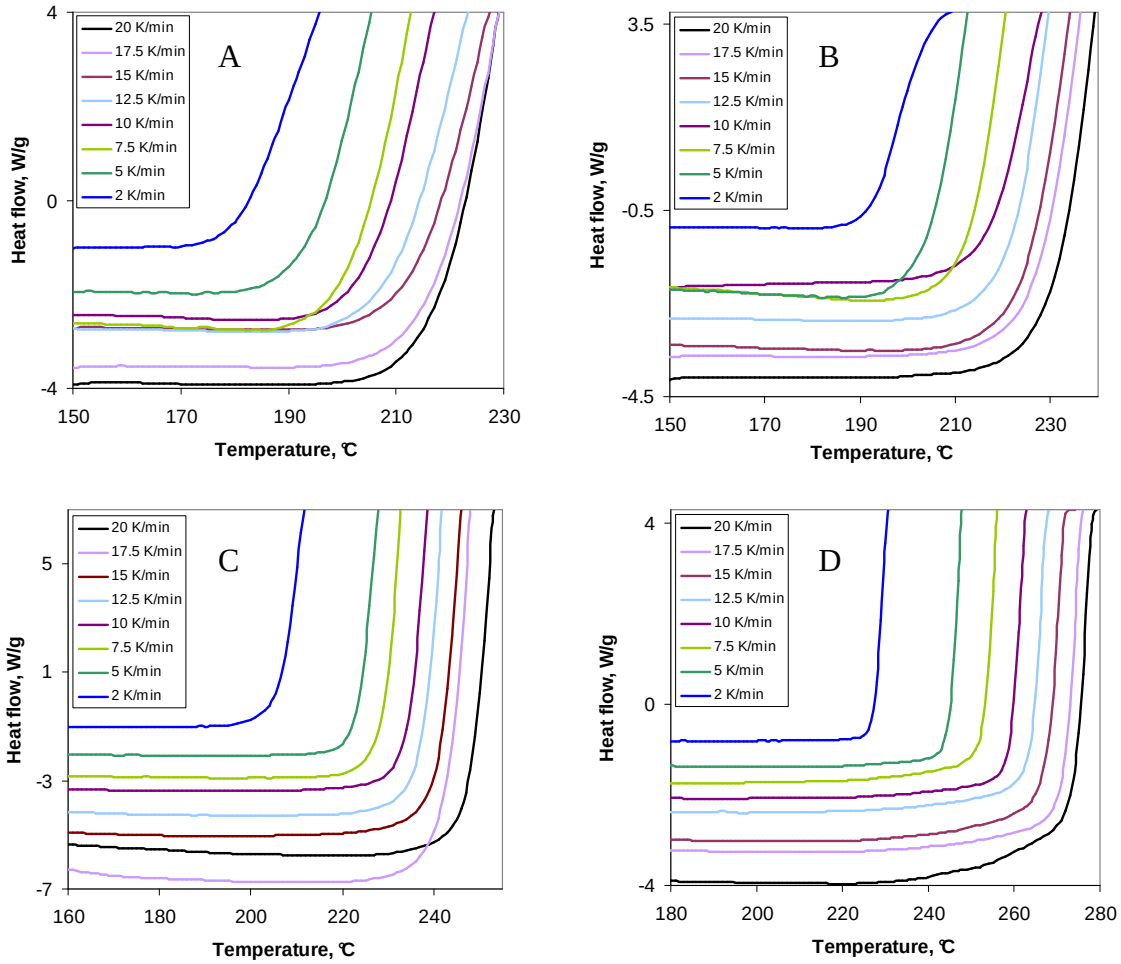

Figure S14. DSC curves of oxidative decomposition of HDPE containing C-ethylcalix[4]pyrogallolarene at concentrations (w/w): A) 0.069%, B) 0.138%, C) 0.276%, D) 1.10%.. All measurements were carried out by DSC in non-isothermal mode at different linear heating rates (β, in $K \cdot min^{-1}$).

Table S6. Temperatures of the extrapolated start (T_e, in K) of oxidation of HDPE composites containing C-ethylcalix[4]pyrogallolarene. The decomposition was monitored at different linear heating rates (β).

β / K·min^{-1}	C-ethylcalix[4]pyrogallolarene concentration [a]				
	0.069% [a]	0.138%	0.276%	0.552%	1.104%
2	454.0	463.4	479.0	490.4	500.4
5	467.5	477.5	495.8	505.1	517.5
7.5	474.6	485.4	501.5	512.1	525.2
10	477.9	489.6	506.3	517.9	531.1
12.5	480.9	493.6	509.8	521.3	535.6
15	485.2	496.4	512.5	525.6	539.5
17.5	488.0	498.2	515.7	528.6	543.4
20	489.5	501.6	518.7	531.6	544.9

[a] In % (w/w).

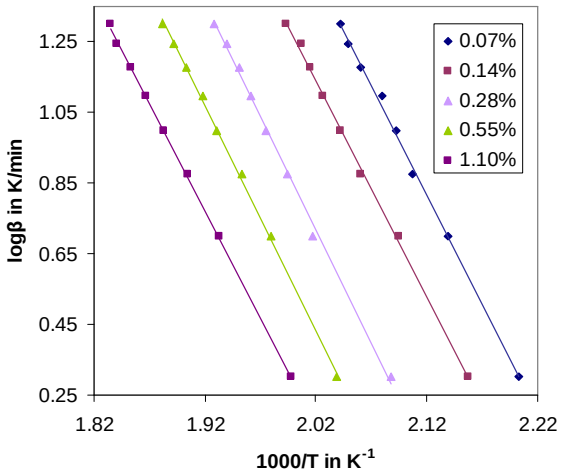

Figure S15. Plots of equation 3 for HDPE composite containing C-ethylcalix[4]pyrogallolarene.

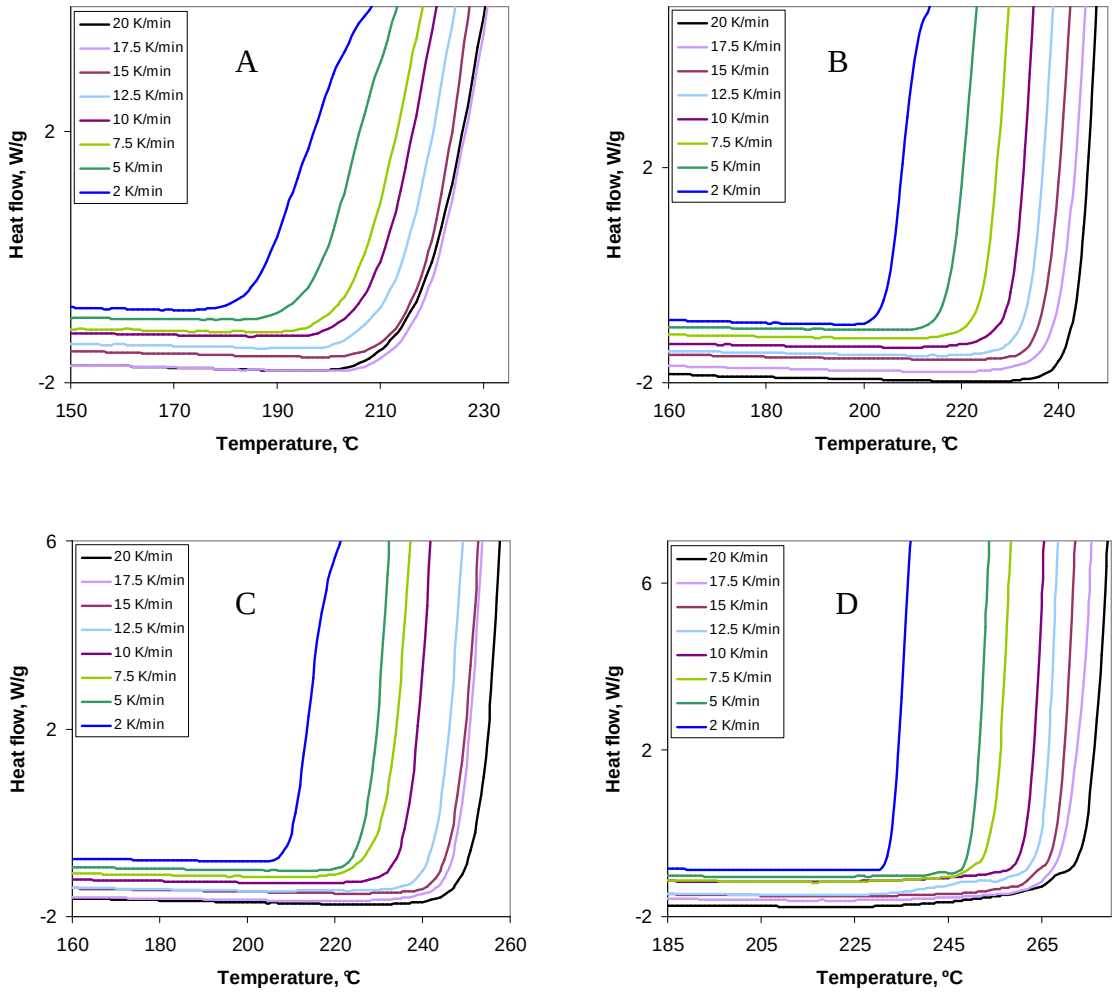

Figure S16. DSC curves of oxidative decomposition of HDPE containing C-undecylcalix[4]pyrogallolarene at concentrations (w/w): A) 0.122%, B) 0.244%, C) 0.488%, D) 1.95%. All measurements were carried out by DSC in non-isothermal mode at different linear heating rates (β, in $K \cdot min^{-1}$).

Table S7. Temperatures of the extrapolated start (T_e, in K) of oxidation of HDPE composites containing C-undecylcalix[4]pyrogallolarene. The decomposition was monitored at different linear heating rates (β, in $K \cdot min^{-1}$).

β / $K \cdot min^{-1}$	C-undecylcalix[4]pyrogallolarene concentration [a]				
	0.122% [a]	0.244%	0.488%	0.976%	1.952%
2	458.0	477.3	483.3	495.3	506.1
5	469.6	490.1	500.1	513.0	523.5
7.5	478.4	497.2	504.8	516.8	527.8
10	481.9	503.1	510.1	522.3	534.8
12.5	486.0	507.4	516.6	529.1	537.7
15		510.7	520.2		541.2
17.5	490.4	513.8	521.5	535.9	543.1
20	491.7	515.7	525.0	540.3	546.4

[a] In % (w/w).

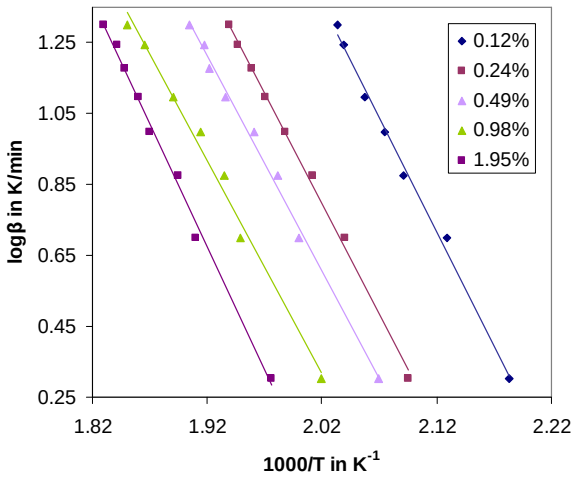

Figure S17. Plots of equation 3 for HDPE composite containing C-undecylcalix[4]pyrogallolarene.

Table S8. Parameters of equation 3, overall activation energies (E_a / kJ·mol^{-1}) and logarithms of pre-exponential factors (Z / s^{-1}), logarithms of overall rate constants for oxidation at 150°C, 200°C, 250°C (k / s^{-1}) calculated for HDPE containing cyclic tetramers. Concentrations of inhibitors in % (w/w).

Concentration of inhibitor	*a*	*b*	R^2	E_a [a]	log*Z*	log$k_{(150°C)}$	log$k_{(200°C)}$	log$k_{(250°C)}$
C-methylcalix[4]pyrogallolarene								
0.063	-5.54	12.45	0.9955	101±5	10.68	-3.54	-2.23	-1.16
0.127	-6.16	13.47	0.9993	112±3	11.65	-3.97	-2.51	-1.32
0.254	-6.85	14.30	0.9972	125±5	12.44	-4.73	-3.10	-1.79
0.508	-7.40	15.16	0.9983	135±5	13.26	-5.14	-3.38	-1.96
1.02	-6.11	12.48	0.9901	111±9	10.67	-4.85	-3.40	-2.22
C-ethylcalix[4]pyrogallolarene								
0.069	-6.23	14.03	0.9978	113±4	12.21	-3.58	-2.10	-0.90
0.138	-6.13	13.52	0.9986	111±4	11.70	-3.84	-2.39	-1.21
0.276	-6.43	13.70	0.9973	117±5	11.87	-4.36	-2.83	-1.60
0.552	-6.34	13.23	0.9988	115±3	11.41	-4.61	-3.11	-1.89
1.10	-6.05	12.40	0.9995	110±2	10.59	-4.79	-3.36	-2.19
C-undecylcalix[4]pyrogallolarene								
0.122	-6.44	14.36	0.9942	117±8	12.53	-3.71	-2.19	-0.95
0.244	-6.23	13.38	0.9968	113±5	11.56	-4.22	-2.74	-1.54
0.488	-6.08	12.89	0.9944	111±7	11.08	-4.37	-2.92	-1.75
0.976	-6.04	12.52	0.9890	110±10	10.71	-4.65	-3.21	-2.05
1.95	-6.97	14.06	0.9954	127±7	12.19	-5.25	-3.60	-2.26

[a] The errors of the activation energy E_a estimated on the basis of the standard deviations of the slopes (listed in column 2) calculated for confidence level 90%.

APPENDIX[1]

Derivation of the equation 3 (the OFW method).

In thermal analysis the rate law for the process is defined as:

$$\frac{d\alpha}{d\tau} = k(\mathrm{T}) \times f(\alpha) \tag{S1}$$

where α is a degree of conversion, τ is time, k(T) is a rate constant and f(α) is a function describing kinetic model of reaction.[2] Rate constant k(T) is given by Arrhenius equation:

$$k(\mathrm{T}) = Z \times e^{-\frac{E_a}{\mathrm{R\,T}}} \tag{S2}$$

By combination of equations S1 and S2 the equation S3 is obtained in logarithmic form:

$$\ln \frac{\frac{d\alpha}{d\tau}}{f(\alpha)} = \ln Z + \left(-\frac{E_a}{R}\right)\left(\frac{1}{T}\right) \tag{S3}$$

Therefore, a calculation of the kinetic parameters E_a and Z is based on the plotting of a linear dependence $\ln[(d\alpha/d\tau)/f(\alpha)]$ as a function of $1/T$.

When measurements are carried out under non-isothermal conditions (a sample is heated with linear heating rate $\beta = \mathrm{d}T/\mathrm{d}\tau$, the equation S1 is modified to describe the changes of α as a function of increasing temperature:

$$\frac{d\alpha}{dT} = \frac{1}{\beta}\frac{d\alpha}{dT} = \frac{Z}{\beta}\exp\left(-\frac{E_a}{RT}\right) f(\alpha) \tag{S4}$$

Separation of variables in equation S4 leads to equation:

$$\frac{d\alpha}{f(\alpha)} = \frac{Z}{\beta}\exp\left(-\frac{E_a}{RT}\right) dT \tag{S5}$$

From this equation two kinds of methods, differential and integral, can be evaluated for determination of kinetic parameters. In differential methods (the Carrol and Manche method, the Freeman and Carrol method) the experimental data are put directly into equation S5, whereas integration of that equation is a basis of the integral methods:

$$g(\alpha) = \int_{T_0}^{T} \frac{d\alpha}{f(\alpha)} = \int_{T_0}^{T} \left[\frac{Z}{\beta}\exp\left(-\frac{E_a}{R}\right)\right] dT \tag{S6}$$

where T_o is a temperature of start of the process. Calculation of the integral form of g(α) with substitution $x = E_a / RT$ yields the expression:

$$\frac{1}{\beta}\int_{T_0}^{T} \exp\left(\frac{-E_a}{RT}\right)\mathrm{d}T = \frac{E_a}{R}\int_{x_0}^{x} \frac{\exp(-x)}{x^2}\mathrm{d}x = \left[\frac{\exp(-x)}{x} - \int_{x}^{\infty}\frac{\exp(-x)}{x^2}\mathrm{d}x\right]_{x_0}^{x} = p(x) \tag{S7}$$

For x >20 the approximation $\log p(x)$ =-2.315 - 0.4567x was proposed by Doyle[3] and this expression was introduced to the equation S6 by Ozawa[4] and, independently, by Flynn and Wall[5] (1966). For given degree of conversion (for example, temperature of start of the process or temperature of maximal heat flow) a plot of $\log \beta$ vs. T^{-1} gives a straight line:

$$\log \beta = (-0.4567\, E_a / \mathrm{R}T) - 2.315 + \log (Z E_a / R) \tag{S8}$$

Activation energy can be calculated from the slope and preexponential factor Z can be calculated from the intercept of eq. S8 (equation 3 in the manuscript text).

---

[1] Litwinienko, G. *Analysis of Lipid Oxidation by Differential Scanning Calorimetry*. In *Analysis of Lipid Oxidation*; AOCS Publishing, **2005**.

2 One of the most frequently used model is: $f(\alpha) = (1-\alpha)^n$ where n is order of reaction. Usually, for autocatalytic reactions $f(\alpha) = \alpha(1-\alpha)^n$ The relatively simple forms of f(α) for model of n-th order reaction (see Table 3) have n = 0, 1, 2 or simply 1/2, 2/3 etc.

3 Doyle, C. D. *J. Appl. Polymer. Sci.*, **1961**, *5*, 285-292. Doyle, C. D. *Nature* **1965**, *207*, 290-291.

4 Ozawa, T. *Bull. Chem. Soc. Jpn.*, 1965, 38, 1881-1885, Ozawa, T. *J. Therm. Anal.* 1970, 2, 301 - 324.

5 Flynn, J. H., and Wall, L. A. *J. Polym. Sci. B, Polym. Letters* **1966**, *4*, 323-328.

Derivation of the overall rate constant for hydrocarbon oxidation.

Autoxidation is a chain process that can be described by the following sequence of reactions:

initiation	Initiator	$\rightarrow$	$R^{\bullet}$	R_i; k_i	(S9)
propagation	$R^{\bullet} + O_2$	$\rightarrow$	$ROO^{\bullet}$	υ_{p1}; k_{p1}	(S10)
	$ROO^{\bullet}+RH$	$\rightarrow$	$R^{\bullet} + ROOH$	υ_{p2}; k_{p2}	(S11)
termination	$ROO^{\bullet}+ ROO^{\bullet}$	$\rightarrow$	$(ROO)_2$	υ_{t1}; k_{t1}	(S12)
	$R^{\bullet} + ROO^{\bullet}$	$\rightarrow$	R-O-R	υ_{t2}; k_{t2}	(S13)
	$R^{\bullet} + R^{\bullet}$	$\rightarrow$	R-R	υ_{t3}; k_{t3}	(S14)

where R_i is a rate of initiation and υ_i, k_i denote rate and rate constant of i-th reaction, respectively.
If a stationary state is reached and if the kinetic chains of propagation are long enough, the rate of initiation (R_i) and a sum of rates of terminations are equal,

$$R_i = 2\,k_{t1}[ROO^{\bullet}]^2 + 2\,k_{t2}[R^{\bullet}]\,[ROO^{\bullet}] + 2\,k_{t3}[R^{\bullet}]^2 \qquad \text{(S15)}$$

and $k_{p1}[R^{\bullet}][O_2] = k_{p1}[ROO^{\bullet}][RH]$.The rate of oxidation can be described as:

$$\upsilon = \frac{k_{p1}k_{p2}[RH][O_2]\sqrt{R_i}}{\sqrt{2k_{t1}k_{p1}^2[O_2]^2 + 2k_{t2}k_{p1}k_{p2}[O_2][RH] + 2k_{t3}k_{p2}^2[RH]^2}} \qquad \text{(S16)}$$

For relatively high oxygen pressure (>13 kPa):

$$k_{t1}k_{p1}^2[O_2]^2 >> k_{t2}k_{p1}k_{p2}[O_2][RH] + k_{t3}k_{p2}^2[RH] \qquad \text{(S17)}$$

and the rate of oxidation (equation S16) can be simplified to the form:[6]

$$\upsilon = k_{p2}\sqrt{\frac{R_i}{2k_{t1}}}[RH] \qquad \text{(S18)}$$

The abstraction of a hydrogen from hydrocarbon is a rate determining step and autoxidation is a first order process with respect to lipid. According to this equation a determination of any parameter related to υ can be used for monitoring the extent of reaction. Since the heat evolved during oxidation is an analytical signal, calorimetry is a valuable tool to follow the oxidation course. During the initial stage of oxidation [RH] is assumed to be constant, and the rate of initiation R_i is effectively constant. Therefore,

$$k_{p2}\sqrt{\frac{R_i}{2k_{t1}}}[RH] = k = \text{const} \qquad \text{(S19)}$$

and k is a global (overall) rate constant of first order reaction.[7]

[6] Lucarini, M.; Pedulli, G. F. *Chem. Soc. Rev.* **2010**, *39*, 2106-2119.
[7] Garcia-Ochoa, F., Romero, A., and Querol, J. *Ind. Eng. Chem. Res.* **1989**, *28*, 43. Jensen, R. K., Korcek, S., Mahoney, L. R., and Zinbo, M. *J. Am. Chem. Soc.* **1981**, *103*, 1742-1749.